Proton NMR Study of Cobalt(II) and Zinc(II) 'Jellyfish' Type Porphyrins

YOSHIO UEMORI and EISHIN KYUNO*

School of Pharmacy, Hokuriku University, 3-Ho, Kanagawa Machi, Kanazawa (Japan)

(Received October 20, 1989; revised February 26, 1990)

Abstract

Proton NMR spectra for 'jellyfish' type porphyrinatocobalt(II) and zinc(II) complexes were measured. Upon complexing with cobalt(II), ^{1}H NMR spectra of the porphyrin ligands suggest the deformations of the cavity structures, while such deformations were not observed in the case of Zn(II) complexes. Proton NMR spectra for the various axial base adducts of the Zn(II) complexes were measured in both toluene-d_8 and $CDCl_3$, and the equilibrium constants for axial base bindings to the Zn(II) complexes were also measured spectrophotometrically. The Zn(II) complexes having fence structures show significant changes in the ^{1}H NMR spectra upon binding with bulky axial bases such as piperidine. These observations suggest that the porphyrin rings can be deformed by the binding of axial bases, and they can be explained in terms of unfavorable steric repulsions between the fence structures and the bound axial bases. Temperature dependence of 1,2-dimethylimidazole (diMeIm) adducts of the Zn(II) complexes were measured. Solution behaviours of diMeIm bound to Zn(II) complexes and of the porphyrin ligands are also discussed.

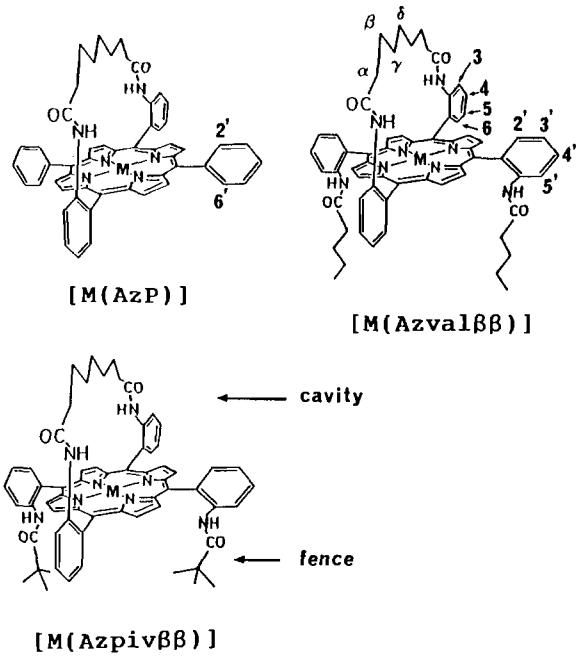

Fig. 1. 'Jellyfish' type porphyrinato complexes and labelling scheme (M = Co, Fe, Zn).

Introduction

In the previous paper [1], we reported that O_2 affinities of 'jellyfish' type porphyrinatoCo(II) complexes (Fig. 1) vary with the fence structures, although these complexes have essentially the same structures around the O_2 binding site (cavity). The O_2 affinities of the complexes in toluene containing an axial base tend to be in the order of [Co(AzP)] > [Co(Azvalββ)] > [Co(Azpivββ)]. On the other hand, O_2 and CO affinities of the corresponding Fe(II) complexes were found to decrease in the order [Fe(Azvalββ)] > [Fe(AzP)] > [Fe(Azpivββ)] [2]. From the measurements of ^{1}H NMR spectra for both O_2 and CO adducts of the Fe(II) complexes, it was found that the cavity conformations in both O_2 and CO adducts of [Fe(Azpivββ)(1,2-dimethylimidazole)] differ from those of the other two complexes and that the cavity conformation in the O_2 adduct of [Fe(Azvalββ)(1,2-dimethylimidazole)] is also different from those of the other two complexes [2]. Because the corresponding porphyrin ligands exhibit virtually identical ^{1}H NMR spectra for the cavity protons [1], the cavity conformation is suggested to change at one of the following processes: the formation of Fe(II) complexes, forming the base adducts of the Fe(II) complexes and forming O_2 or CO adducts of these complexes.

This study has been done to elucidate the factors affecting the conformation of cavities in 'jellyfish' porphyrins and in the metal complexes. Diamagnetic Zn(II) complexes of the porphyrins were prepared to investigate the behavior of the porphyrins in solution by NMR spectroscopy. The ^{1}H NMR spectra of the porphyrins, Zn(II) complexes and Co(II) complexes were recorded to determine the

*Author to whom correspondence should be addressed.

0020-1693/90/$3.50

changes of cavity conformation upon formation of Zn(II) or Co(II) complexes. Changes in the cavity conformation upon binding of the axial bases to the Zn(II) or Co(II) complexes were also monitored by ^{1}H NMR spectroscopy. The equilibrium constants for the axial base bindings to Zn(II) complexes were determined spectrophotometrically.

Experimental

Measurements

Electronic spectra were recorded on a Hitachi 340 spectrophotometer. Equilibrium constants for the axial base bindings to the Zn(II) complexes in $CHCl_3$ were determined by spectrophotometric titration as described previously [1]. Proton NMR spectra were recorded on a JEOL GSX-400 spectrometer. Variable-temperature NMR spectra were obtained on a JEOL GSX-400 with the use of a standard JEOL constant-temperature controller. Each NMR sample was allowed to equilibrate for 15 min in the spectrometer before data were collected.

Materials

Piperidine (pip), 1-methylimidazole (1-MeIm), and 1,2-dimethylimidazole (diMeIm) were vacuum distilled from KOH. Benzimidazole (BzIm) was recrystallized from benzene. Chloroform (HPLC grade) was purified by passage through a column of activated alumina just before use. 1,5-Dicyclohexylimidazole (DCIm) was prepared by the method of Traylor *et al.* [3]. 'Jellyfish' type porphyrins and the Co(II) complexes were prepared as described before [1]. [Zn(AzP)] was prepared by the method reported previously [4].

Zn(II) Insertion

Zn(II) complexes were prepared by heating the porphyrins with $Zn(CH_3COO)_2 \cdot 4H_2O$ in MeOH at 50 °C for 1 h. Purification was accomplished with a silica gel column using CH_2Cl_2/ether (4:1 vol./vol.) as eluent.

[Zn(Azvalββ)]

Anal. Calc. for $C_{62}H_{60}N_8O_4Zn \cdot 2H_2O$: C, 69.38; H, 5.55; N, 10.27. Found: C, 69.71; H, 5.39; N, 10.28%.

[Zn(Azpivββ)]

Anal. Calc. for $C_{62}H_{60}N_8O_4Zn \cdot 3H_2O$: C, 68.38; H, 5.47; N, 10.13. Found: C, 68.52; H, 5.27; N, 9.99%.

Results and Discussion

In the interpretation of the changes in O_2 affinities for 'jellyfish' type porphyrinatoCo(II) complexes, we assumed that the cavity conformations do not change among the complexes [1]. As stated above, this assumption was found to be incorrect for the Fe(II) complexes. Therefore, ^{1}H NMR spectra for 'jellyfish' type porphyrins were reexamined by using a 400 MHz NMR instrument. As shown in the previous work using a 100 MHz NMR instrument [1], the heptamethylene (C-7 chain) protons of each porphyrin resonate at nearly identical chemical shifts (±0.02 ppm) in $CDCl_3$ (Table 1). Changing the solvent from $CDCl_3$ to toluene-d_8, the signals of both phenyl and C-7 chain protons shift more than 0.4 ppm compared with those measured in $CDCl_3$. Furthermore, the signals of the amide protons in fences shift to higher field and those of N-H protons in pyrroles shift to lower field compared with the corresponding signals which appeared in $CDCl_3$. Because these changes in signals are observed among the three porphyrins, the solvent dependence may not be due to an interaction of the fences with toluene, but may be due to the formation of π-complexes between porphyrins and toluene [5–7].

^{1}H NMR Spectra for the Co(II) Complexes

Proton NMR spectra for 'jellyfish' type porphyrinatocobalt(II) complexes were measured in both toluene-d_8 and $CDCl_3$. The ^{1}H NMR spectra of the Co(II) complexes appear in the range of more than 50 ppm, due to the paramagnetic interaction with the Co(II) center as seen in Table 2. The C7-chain proton signals differ among the four-coordinated Co(II) complexes in toluene-d_8. Although the resonances due to the C7-chain protons in both [Co(AzP)] and [Co(Azvalββ)] are almost identical in $CDCl_3$, they are different from those of [Co(Azpivββ)]. It is difficult to evaluate the ^{1}H NMR data for the Co(II) complexes because of the solvent effect and the paramagnetic contribution of Co(II). However, the differences in the δ proton signals between [Co(Azpivββ)] and the other complexes are comparable to those observed for the Co(II) complexes of 'cap' porphyrins having different size of caps [8, 9]. Thus, the changes in the δ proton signals of the Co(II) complexes in $CDCl_3$ are significant. Therefore, it is concluded that the cavity conformation of [Co(Azpivββ)] in $CDCl_3$ is changed upon Co(II) insertion.

Addition of 1-methylimidazole (1-MeIm) to [Co(Azpivββ)] under Ar produces the base adduct, [Co(Azpivββ)(1-MeIm)]; its spectrum is shown in Fig. 2. The resonances appearing at higher field than 0 ppm can be assigned to the C-7 chain protons [8, 10, 11]: −3.0, −1.3 and −0.1 ppm for [Co(AzP)(1-MeIm)]; −3.1, −1.4 and −0.5 ppm for [Co(Azvalββ)(1-MeIm)]; −3.2, −1.5 and −0.7 ppm for [Co(Azpivββ)(1-MeIm)]. Assignment of the amide protons cannot be made in the ^{1}H NMR spectra of the Co(II) complexes; however, it can be concluded that the cavity conformations in the Co(II) complexes are not identical in both the four-coordi-

TABLE 1. Solvent dependence of the chemical shifts in 'jellyfish' type porphyrins[a]

	H_2-AzP		H_2-Azval$\beta\beta$		H_2-Azpiv$\beta\beta$	
	$CDCl_3$	Toluene-d_8	$CDCl_3$	Toluene-d_8	$CDCl_3$	Toluene-d_8
δ	−2.50	−2.80	−2.51	−2.77	−2.52	−2.82
γ	−0.50	−0.91	−0.52	−0.92	−0.54	−0.95
β	−1.22	−1.40	−1.25	−1.41	−1.25	−1.46
α	+1.16	+0.91	+1.20	+0.89	+1.18	+0.90
Amide	6.00	6.04	5.95	5.91	5.93	5.92
			6.52	6.34	7.01	[b]
3	8.46	8.92	8.42	9.09	8.42	9.15
4	7.66	7.64	7.68	7.59	7.68	7.59
5	7.84	7.38	7.85	7.24	7.85	7.22
6	8.35	8.26	8.33	7.84	8.34	7.76
2′	8.06	7.93	8.07	8.19	8.07	8.13
3′	7.81	7.41	7.57	7.34	7.57	7.35
4′	7.75	7.49	7.87	7.61	7.87	7.61
5′	7.81	7.47	8.68	8.84	8.66	8.84
6′	8.28	8.05				
Pyrrole	8.88	8.77	8.85	8.71	8.87	8.70
	8.81	8.75		8.69	8.83	
N–H	−2.65	−2.35	−2.61	−2.23	−2.56	−2.22
Fence			1.29	0.71	0.14	0.00
			0.78	0.58		
			0.53	0.25		
			0.15	0.02		

[a]Chemical shifts (δ) at 24 °C. For the labelling system, see Fig. 1. [b]Signal was not assigned.

TABLE 2. Solvent dependence of ^1H NMR signals for heptamethylene protons in 'jellyfish' type Co(II) porphyrins[a]

	[Co(AzP)]		[Co(Azval$\beta\beta$)]		[Co(Azpiv$\beta\beta$)]	
	Toluene-d_8	$CDCl_3$	Toluene-d_8	$CDCl_3$	Toluene-d_8	$CDCl_3$
δ	[b]	−25.0	[b]	−25.0	−38.1	−30.2
γ	−14.3	−12.2	−16.1	−12.3	−17.4	−14.2
β	−10.1	−9.2	−12.2	−9.4	−13.3	−11.2
α	−5.7	−5.7	−6.6	−5.4	−7.2	−6.0

[a]Chemical shifts (δ) at 24 °C. Concentrations of Co(II) complexes were *c.* 0.2 and 2 mM in toluene-d_8 and $CDCl_3$, respectively. The letters (δ–α) refer to the positions in heptamethylene (see Fig. 1). [b]Signals were not assigned.

nated Co(II) complexes and their base adducts. Thus, the changes in the O_2 affinities for 'jellyfish' type porphyrinatoCo(II) complexes may be due to the changes in the cavity structure as reported in the corresponding Fe(II) complexes [2]. The O_2 adduct of [Co(Azpiv$\beta\beta$)] is prepared by passing O_2 gas into a solution of the base adduct (Fig. 3). In the spectra of the O_2 adducts, the C-7 chain protons resonate in a narrow range (from *c.* 1 to −1 ppm). This observation may be due to the shift of an unpaired d-electron from Co(II) to the bound O_2 molecule as discussed in the ESR studies [12]. In agreement with our observation, it has been reported that the ^1H NMR signals were not observed in low field for the O_2 adduct of cobalt-hybrid hemoglobin [13]. As the C-7 chain proton signals of the O_2 adducts are complicated it is impossible to discuss details of the cavity structures at present.

^1H NMR Spectra for the Zn(II) Complexes

From the results on the Co(II) complexes, it is concluded that 'jellyfish' type porphyrins have not

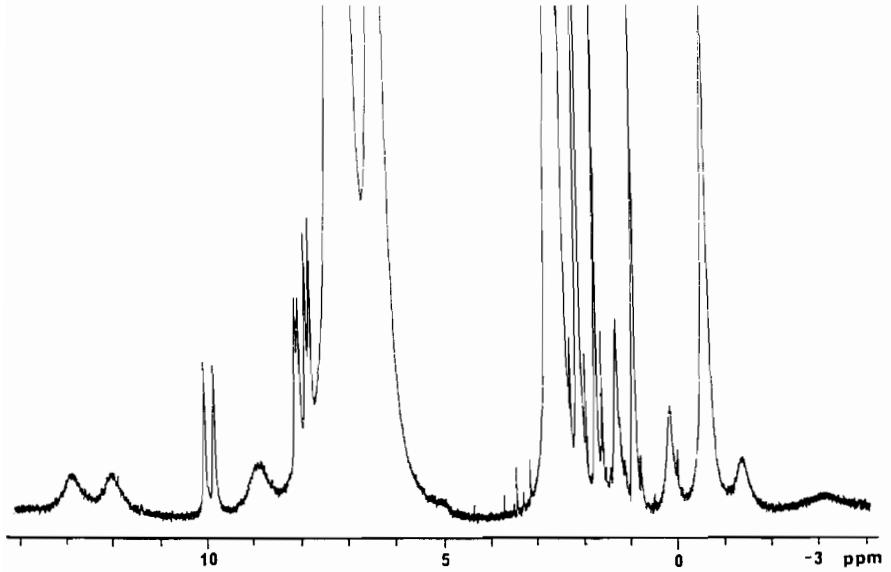

Fig. 2. ^{1}H NMR spectrum of [Co(Azpiv$\beta\beta$)] (*c.* 1.6 mM) in toluene-d_8 containing 1-methylimidazole (0.1 M) at 24 °C.

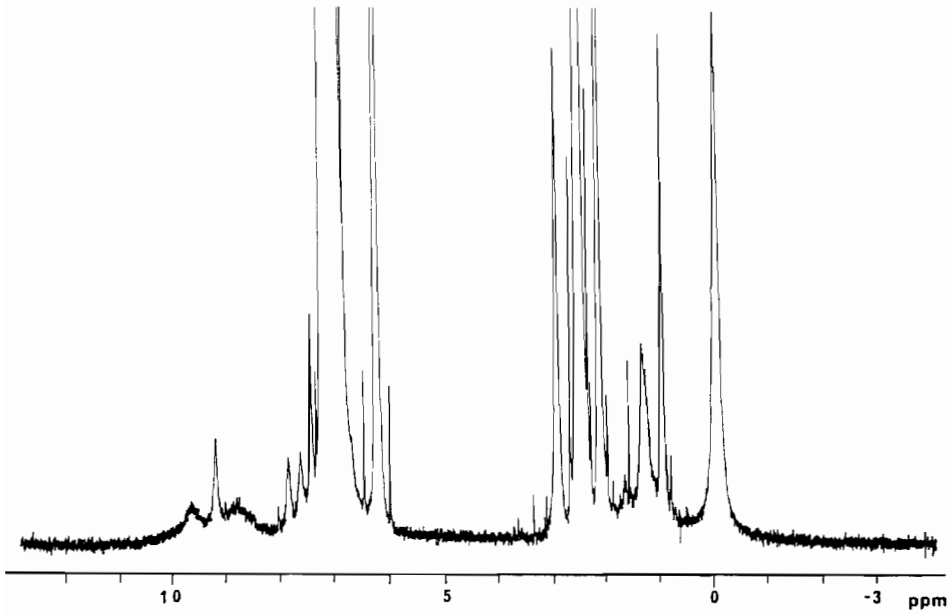

Fig. 3. ^{1}H NMR spectrum of the O_2 adduct of [Co(Azpiv$\beta\beta$)] (*c.* 1.6 mM) in toluene-d_8 containing 1-methylimidazole (0.1 M) at −20 °C.

the same cavity conformations in the Co(II) complexes as in the Fe(II) analogues [2]. In agreement with our results, X-ray studies have shown that porphyrins are deformed by the binding of axial ligands such as CN [14] and CO [15]. Thus, we extended our ^{1}H NMR work to Zn(II) complexes of the porphyrins to obtain information on deformation of porphyrin planes and also on the interactions between fences and axial bases.

Because of the low solubilities of the Zn(II) complexes in toluene-d_8, the ^{1}H NMR spectra were recorded in $CDCl_3$ (Tables 3–5). The shifts of the signals appear for the C7-chain protons in [Zn(AzP)] upon Zn(II) insertion (Fig. 4). In addition to the changes of C7-chain protons, the fence protons including amide protons also shift in both [Zn(Azval$\beta\beta$)] and [Zn(Azpiv$\beta\beta$)]. However, these shifts in the cavity protons (C-7 chain protons and appended amide protons) are smaller than 0.2 ppm. Thus, it means that the cavity conformations are not significantly affected by Zn(II) insertions. It is clear that the cavity conformations are affected by

TABLE 3. ^{1}H NMR data for [Zn(AzP)] and its base adducts[a]

	None	1-MeIm	BzIm	diMeIm	DCIm	pip
δ	−2.65	−2.60	−2.60	−2.63	−2.57	−2.71
γ	−0.50	−0.53	−0.52	−0.53	−0.51	−0.57
β	−1.36	−1.27	−1.25	−1.29	−1.25	−1.35
α	+1.17	+1.12	+1.15	+1.11	+1.12	+1.10
Amide	6.05	6.04	6.09	6.06	6.07	5.99
3	8.43	8.41	8.40	8.39	8.41	8.42
4	7.66	7.59	[b]	7.58	7.59	7.62
5	7.84	7.79	[b]	7.79	7.79	7.81
6	8.37	8.40	8.37	8.39	8.39	8.39
2′	8.12	8.06	[b]	8.06	8.04	8.09
3′	7.8	7.69	[b]	7.68	7.76	7.77
4′	7.75	7.76	[b]	7.74	7.70	7.73
5′	7.8	7.69	[b]	7.68	7.76	7.77
6′	8.25	8.25	8.25	8.23	8.27	8.22
Pyrrole	9.00	8.85	8.88	8.85	8.85	8.89
	8.91	8.74	8.77	8.73	8.73	8.77

[a]Chemical shifts (δ) in $CDCl_3$ at 24 °C. For the labelling system, see Fig. 1. [b]Signals were not assigned.

TABLE 4. ^{1}H NMR data for [Zn(Azvalββ)] and its base adducts[a]

	None	1-MeIm	BzIm	diMeIm	DCIm	pip
δ	−2.62	−2.68	−2.57	−2.64	−2.73	−2.97
γ	−0.53	−0.56	−0.51	−0.54	−0.57	−0.66
β	−1.36	−1.32	−1.24	−1.29	−1.38	−1.55
α	+1.10	+1.13	+1.17	+1.14	+1.15	+1.13
Amide[b]	5.94	6.01	6.05	6.01	6.03	5.92
	6.51	6.60	6.20	6.51	6.68	7.3
3	8.37	8.39	8.37	8.38	8.41	8.37
4	7.66	7.61	[c]	7.61	7.62	7.63
5	7.84	7.79	[c]	7.83	7.79	7.83
6	8.27	8.38	8.35	8.38	8.34	8.37
2′	8.04	8.02	8.1	8.05	7.98	7.75
3′	7.55	7.51	[c]	7.52	7.51	7.45
4′	7.82	7.81	[c]	7.82	7.83	7.8
5′	8.52	8.66	8.5	8.65	8.69	8.7
6′						
Pyrrole	8.91	8.76	8.8	8.77	8.79	8.82
				8.78	8.77	8.79
Fence	0.07	0.29	−0.25	0.36	0.40	0.58
	0.43	0.42		0.50	0.58	0.89
	0.62	0.62	+0.9	0.66	0.73	1.25
	1.10	0.87		0.79	0.89	1.41

[a]Chemical shifts (δ) in $CDCl_3$ at 24 °C. For the labelling system, see Fig. 1. [b]Upper and lower column are for the amide proton signals in cavity and fence structure, respectively. [c]Signals were not assigned.

TABLE 5. ^{1}H NMR data for [Zn(Azpivββ)] and its base adducts[a]

	None	1-MeIm	BzIm	diMeIm	DCIm	pip
δ	−2.70	−2.82	−2.76	−2.75	−2.93	−3.17
γ	−0.53	−0.60	−0.56	−0.58	−0.65	−0.76
β	−1.38	−1.44	−1.38	−1.37	−1.53	−1.71
α	+1.18	+1.15	+1.19	+1.15	+1.15	+1.11
Amide[b]	5.97	6.03	6.09	6.03	6.06	5.94
	7.20	7.39	7.14	7.35	7.65	8.22
3	8.40	8.40	8.41	8.4	8.42	8.38
4	7.68	7.63	7.64	7.62	7.63	7.62
5	7.87	7.78	7.84	7.8	7.78	7.83
6	8.35	8.38	8.39	8.33	8.31	8.33
2′	8.00	7.90	7.91	7.91	7.83	7.50
3′	7.56	7.47	7.47	7.47	7.47	7.38
4′	7.85	7.84	7.75	7.83	7.84	7.79
5′	8.77	8.73	8.63	8.73	8.75	8.85
6′						
Pyrrole	8.99	8.81	8.79	8.80	8.81	8.85
	8.94	8.70	8.77	8.77	8.75	8.76
Fence	+0.19	−0.03	−0.56	−0.08	+0.06	+0.64

[a]Chemical shifts (δ) in $CDCl_3$ at 24 °C. For the labelling system, see Fig. 1. [b]Upper and lower column are for the amide proton signals in cavity and fence structure, respectively.

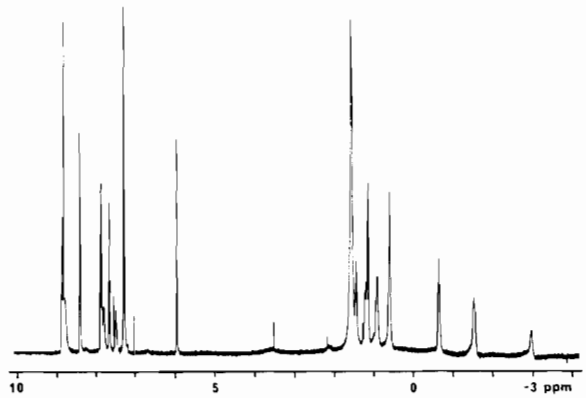

Fig. 4. ^{1}H NMR spectrum of [Zn(Azvalββ)] (*c.* 3.4 mM) in $CDCl_3$ containing piperidine (0.05 M) at 24 °C.

Co(II) insertions, but are not affected by Zn(II) insertions. This may be due to the difference in size between Zn(II) and Co(II). Indeed, Scheidt *et al.* have shown that the porphyrin ring is planar in [Zn(TPP)] [16], but the ring deforms from planarity in [Co(TPP)] [17].

The ^{1}H NMR spectra for the base adducts of Zn(II) porphyrins were obtained by the addition of an excess (*c.* 10 mole equivalent) amount of the bases to the Zn(II) porphyrin solution (*c.* 2 mM)

or suspension. Each signal of the porphyrin ligands in the base adducts of [Zn(AzP)] does not shift more than 0.1 ppm compared with that of [Zn(AzP)], regardless of the axial base employed. On the other hand, the signals of fence protons including the appended amide protons shift significantly upon 1-MeIm binding to the Zn(II) complexes having fence structures. This suggests that the base bindings to Zn(II) occur on the fence side of the porphyrin plane. Furthermore the changes in the chemical shifts of the cavity protons in [Zn(Azpivββ)] become evident as compared with those in both [Zn(AzP)(1-MeIm)] and [Zn(Azvalββ)(1-MeIm)]. This observation is in agreement with the changes of the cavity conformations for the CO adducts of the Fe(II) analogues [2]. A similar trend also appears for the 1,2-dimethylimidazole (diMeIm) adducts of the Zn(II) complexes. Here it is suggested that the changes of the cavity conformations in [Zn(Azvalββ)(diMeIm)] and [Zn(Azpivββ)(diMeIm)] are enlarged by the axial base bindings.

The trend of deviations of the cavity conformations is more evident in the case of the piperidine (pip) adducts. Compared with ^{1}H NMR signals of [Zn(Azvalββ)(1-MeIm)], the signals of C-7 chain protons in [Zn(Azvalββ)(pip)] shift to high fields and those of fence protons including amide protons shift to low fields, although the signals of the phenyl protons carrying the C-7 chain do not shift significantly. Furthermore the signals of both the protons at the 2′- and 3′-position of the phenyls appending the fence structure shift to a higher field and the signals of the protons at the 5′-position shift to a lower field. These changes are more obvious in the case of [Zn(Azpivββ)(pip)] than that of [Zn(Azvalββ)(pip)]. In contrast to this, significant changes in the ^{1}H NMR spectra of [Zn(AzP)] do not appear upon pip binding. Because [Zn(AzP)] does not have a fence structure but both [Zn(Azvalββ)] and [Zn(Azpivββ)] have, it is suggested that there exist steric interactions between the fences and the bound pip. Taking into account the criterion that a proton positioned above the porphyrin ring exhibits a high field shift, the ^{1}H NMR results stated above suggest that both the fence and phenyl groups carrying fences deform as shown in Scheme 1.

Furthermore, the conformation in Scheme 1 is supported by the results of measurements of the

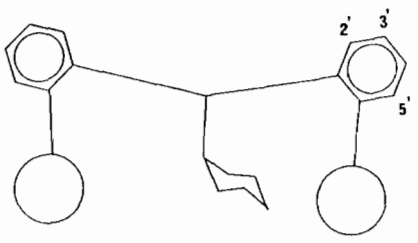

Scheme 1.

equilibrium constants (K_B) for base (B) bindings to the Zn(II) complexes (ZnP). The magnitude of K_B for pip bindings tends to be in the order of

$$[Zn(P)] + B \overset{K_B}{\rightleftharpoons} [Zn(P)(B)]$$

[Zn(AzP)] > [Zn(Azvalββ)] > [Zn(Azpivββ)], although the magnitude for 1-MeIm, pyridine (py), diMeIm or benzimidazole (BzIm) bindings tends to be in the order of [Zn(AzP)] < [Zn(Azvalββ)] < [Zn(Azpivββ)], as shown in Table 6. Because the base bindings to Zn(II) occur on the fence side of the porphyrins, the differences in K_B for pip bindings can be explained as follows. Increasing the bulk of fence structures, the unfavorable steric interactions between the fences and the bound pip will be increased. These interactions may increase in the order of [Zn(AzP] < [Zn(Azvalββ)] < [Zn(Azpivββ)] and the magnitude of K_B for pip bindings decreases in this order. Thus, it may be concluded that the unfavorable steric interactions between the fences and the bound pip induce the deformations of the phenyl groups carrying the fences as shown in Scheme 1. Furthermore, these deformations will follow the second modification of the porphyrin ring which will be responsible for the upfield shift of the C-7 chain protons.

The ^{1}H NMR spectra for 1,5-dicyclohexylimidazole (DCIm) adducts show similar trends as observed for the pip adducts. On the other hand, the changes of the chemical shifts for the C-7 chain protons upon bindings of BzIm to Zn(II) complexes are small and are comparable to those for the 1-MeIm or the diMeIm adducts. The magnitude of K_B for BzIm bindings does not imply an unfavorable steric interaction as observed for the pip adducts. Thus, the small changes of the ^{1}H NMR spectra for the BzIm adducts may be due to the structure in that the BzIm molecules bind to Zn(II) with the molecular plane pointing to the fences as shown in (A) or (B) in Fig. 5. On the contrary, pip molecules bind to [Co(TPP)] in a chair form [18], therefore the molecular plane of pip is thicker than that of BzIm. Thus, steric interactions between the fences and the bound pip may be severe even in the case when pip molecules bind to Zn(II) as shown in (B) in Fig. 5.

TABLE 6. Equilibrium constants (K_B) for base bindings to Zn(II) porphyrins[a]

	1-MeIm	BzIm	diMeIm	DCIm	pip
[Zn(AzP)]	5.8	2.0	7.8	7.7	15
[Zn(Azvalββ)]	10	12	12	3.3	4.1
[Zn(Azpivββ)]	22	16	13	12.5	2.2

[a]Measured in $CHCl_3$ at 25 °C; $K_B \times 10^{-4}$ (M^{-1}); error limits < 20%.

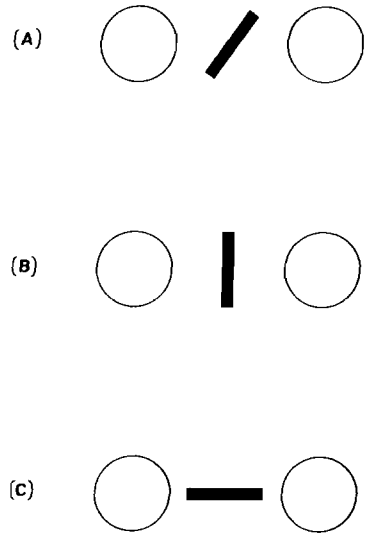

Fig. 5. Schematic representation of the orientation of axial base planes. The circles indicate fence groups and solid rectangles indicate the planes of axial bases.

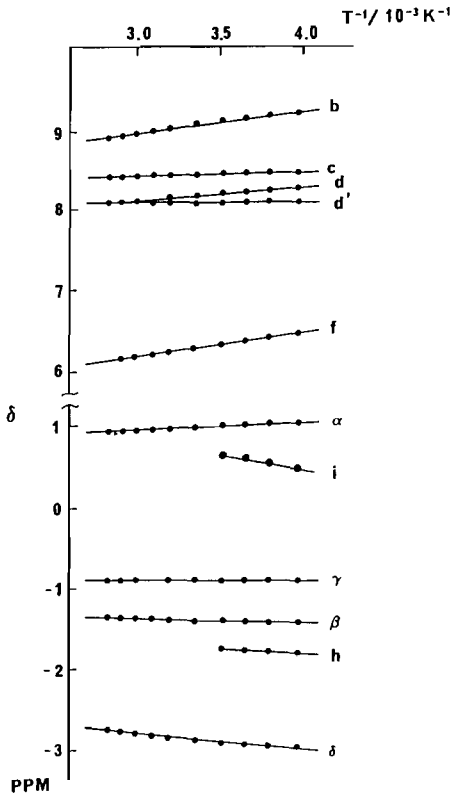

Fig. 6. δ vs. $1/T$ plots of the selected signals for the diMeIm adduct of [Zn(AzP)] in toluene-d_8. The letters (α–δ) refer to the positions of the protons in the heptamethylene chain, see Fig. 1: b = 3H, c = 6-H, d = 2'-H, d' = 6'-H, f = amide-H in a cavity, h = 2-Me in bound diMeIm, i = 1-Me in bound diMeIm.

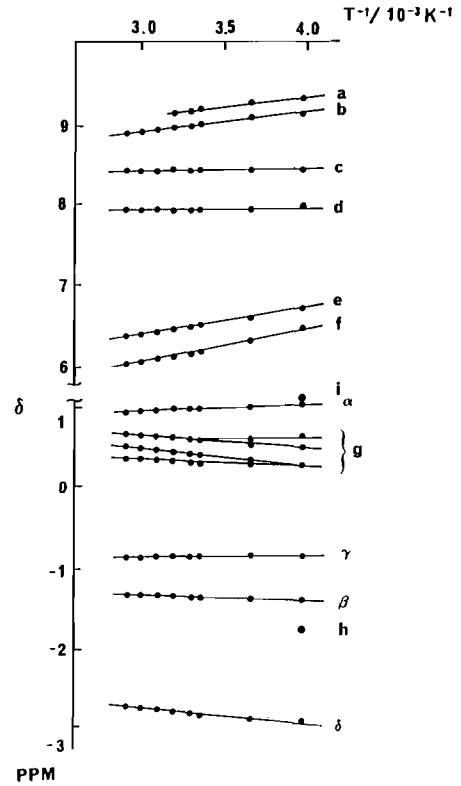

Fig. 7. δ vs. $1/T$ plots of the selected signals for the diMeIm adduct of [Zn(Azvalββ)] in toluene-d_8. a = 5'-H, e = amide-H in fences, g = fence-H, other letters refer to the protons as in Fig. 6.

The signals of the axial bases bound to Zn(II) are not observed at 24 °C, because the concentration of the axial bases are *c.* 10-fold in excess and the ligand exchange may be rapid on the NMR time scale at this temperature. To obtain details on the conformations of the bound base molecules, the temperature dependence of the chemical shifts was measured for the diMeIm adducts of Zn(II) complexes in both toluene-d_8 and $CDCl_3$ (Figs. 6–9). Although the experimental conditions are similar among the three complexes in toluene-d_8, the 2-Me signals of diMeIm bound to Zn(II) appear below 24, 10 and −20 °C for [Zn(Azpivββ)(diMeIm)], [Zn(AzP)(diMeIm)] and [Zn(Azvalββ)(diMeIm)], respectively. The chemical shifts values of the 2-Me signals of the bound diMeIm are virtually identical among the three complexes as shown in Table 7. Furthermore, an indication of splitting of the 2-Me signal in [Zn(Azvalββ)(diMeIm)] is not observed at −60 °C. Thus, any correlation between the chemical shifts of the 2-Me signals and the axial base orientation cannot be deduced. While the chemical shift values of the 1-Me signals of the bound diMeIm are virtually identical among the three complexes in $CDCl_3$, the 1-Me signal of [Zn(AzP)(diMeIm)]

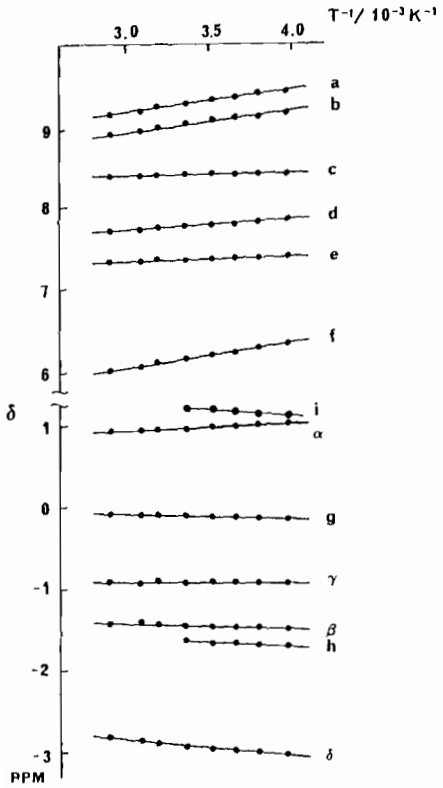

Fig. 8. δ vs. $1/T$ plots of the selected signals for the diMeIm adduct of [Zn(Azpivββ)] in toluene-d_8. The letters refer to the protons as in Fig. 6.

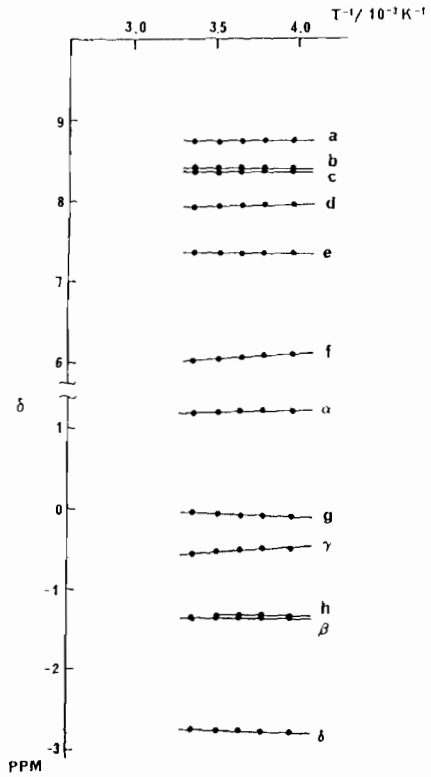

Fig. 9. δ vs. $1/T$ plots of the selected signals for the diMeIm adduct of [Zn(Azpivββ)] in $CDCl_3$. The letters refer to the protons as in Fig. 6.

appears at higher field than those in the other two complexes in toluene-d_8. The 1-Me groups of diMeIm in the diMeIm adducts of Zn(II) complexes locate at the position where the groups can interact with the solvent molecules. Therefore, it is suggested that the bound diMeIm molecule in [Zn(AzP)-(diMeIm)] is exposed to the solvent (toluene-d_8), while the diMeIm molecules are shielded from toluene-d_8 by the fences in both [Zn(Azalββ)-(diMeIm)] and [Zn(Azpivββ)(diMeIm)].

The proton signals at the 2′ and 6′ positions in the phenyl groups of [Zn(AzP)(diMeIm)] appear as two separate doublets at room temperature, reflecting the magnetic none-equivalence of both sides of the porphyrin plane and the restricted rotation on the phenyl groups. As the temperature is raised from 24 to 70 °C, the pair of signals become broad and is observed as one signal. The coalescence temperature for the signals is *c.* 55 °C and is comparable to that observed for [TiO(p-CF_3TTP)]Cl [19]. This coalescence behavior is a result of atropisomerization processes which become rapid on the NMR time scale [20]. In [Zn(Azalββ)(diMeIm)], the signals of the pyrrole protons are broadened and averaged to a doublet and the doublet signal of the protons at the 5′ position in the phenyl groups carrying fence groups are also broadened as the temperature is raised from −20 to 70 °C (Fig. 10).

TABLE 7. The chemical shifts (δ) of 1,2-dimethylimidazole bound to Zn(II) complexes at −20 °C

	1-Methyl protons	2-Methyl protons	Solvent
[Zn(AzP)(diMeIm)]	0.47	−1.79	toluene-d_8
	2.20	−1.36	$CDCl_3$
[Zn(Azalββ)(diMeIm)]	1.0	−1.73	toluene-d_8
	2.21	−1.33	$CDCl_3$
[Zn(Azpivββ)(diMeIm)]	1.11	−1.72	toluene-d_8
	2.21	−1.38	$CDCl_3$

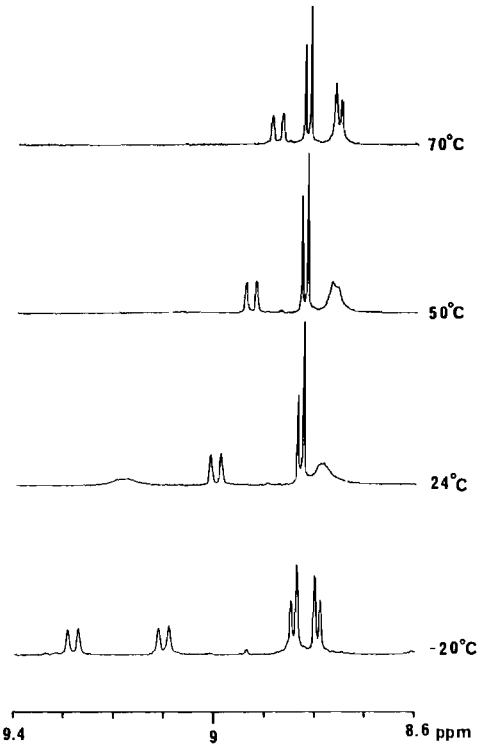

Fig. 10. ^1H NMR spectra of [Zn(Azval$\beta\beta$)] (*c.* 2.7 mM) in toluene-d_8 containing 1,2-dimethylimidazole (0.04 M) at various temperatures.

These two processes will be due to the 'wagging' motion of the phenyl groups. They are not due to rotation of the phenyl groups, because no atropisomer was detected after cooling of the samples at 70 °C. On the other hand, such broadening of the signals does not appear in [Zn(Azpiv$\beta\beta$)(diMeIm)]. Thus, the phenyl groups carrying fence groups in [Zn(Azval$\beta\beta$)(diMeIm)] are found to wag around the porphyrin–phenyl bond.

Interactions between Zn(II) complexes and toluene-d_8 are also evident: the amide protons and the adjacent phenyl protons shift to high fields with a temperature decrease in toluene-d_8. However, such shifts are not observed in $CDCl_3$. Therefore, these shifts may be due to interactions between the complexes and toluene-d_8. The temperature dependence of these signals can be explained in terms of magnetic anisotropy of toluene. The orientated toluene-d_8 molecules which cause the amide signals to shift to high fields may become random with an increase in temperature.

Conclusions

The cavities in 'jellyfish' type porphyrinatoZn(II) complexes have virtually identical conformations. On the other hand, the cavity conformations are different among the corresponding Co(II) complexes and this may be partly responsible for the changes in the O_2 affinities of the Co(II) complexes. The changes of cavity conformations are also induced by the steric repulsions between the axial bases and the fence structures. Hence, it is concluded that the porphyrin skeletons are flexible rather than rigid.

References

1 Y. Uemori, H. Miyakawa and E. Kyuno, *Inorg. Chem., 27* (1988) 377.
2 Y. Uemori and E. Kyuno, *Inorg. Chem., 28* (1989) 1690.
3 T. G. Traylor, S. Tsuchiya, D. Campbell, M. Mitchell, D. Stynes and N. Koga, *J. Am. Chem. Soc., 107* (1985) 604.
4 Y. Uemori and E. Kyuno, *Inorg. Chim. Acta, 165* (1989) 115.
5 N. J. Clayden, G. R. Moore, R. J. P. Williams, J. E. Baldwin and M. J. Crossley, *J. Chem. Soc., Perkin Trans. II,* (1982) 1693.
6 J. F. Kirner, C. A. Reed and W. R. Scheidt, *J. Am. Chem. Soc., 99* (1977) 1093; W. R. Scheidt, M. E. Kastner and K. Hatano, *Inorg. Chem., 17* (1978) 706; W. R. Scheidt and C. A. Reed, *Inorg. Chem., 17* (1978) 710.
7 G. P. Fulton and G. N. LaMar, *J. Am. Chem. Soc., 98* (1976) 2116; G. P. Fulton and G. N. LaMar, *J. Am. Chem. Soc., 98* (1976) 2124.
8 N. J. Clayden, G. R. Moore, R. J. P. Williams, J. E. Baldwin and M. J. Crossley, *J. Chem. Soc., Perkin Trans. II,* (1983) 1863.
9 J. W. Sparapany, M. J. Crossley, J. E. Baldwin and J. A. Ibers, *J. Am. Chem. Soc., 110* (1988) 4559.
10 G. N. LaMar and F. A. Walker, *J. Am. Chem. Soc., 95* (1973) 1790.
11 A. Shirazi and H. M. Goff, *Inorg. Chem., 21* (1982) 3420.
12 T. D. Smith and J. R. Pilbrow, *Coord. Chem. Rev., 39* (1981) 295.
13 M. Ikeda-Saito, T. Inubushi, G. G. McDonald and T. Yonetani, *J. Biol. Chem., 253* (1978) 7134.
14 M. Schappacher, J. Fischer and R. Weiss, *Inorg. Chem., 28* (1989) 390.
15 K. Kim, J. Fettinger, J. L. Sessler, M. Cyr, J. Hugdahl, J. P. Collman and J. A. Ibers, *J. Am. Chem. Soc., 111* (1989) 403.
16 W. R. Scheidt, J. U. Mondal, C. W. Eigenbort, A. Alder and L. J. Radonovich, *Inorg. Chem., 25* (1986) 795.
17 P. Madura and W. R. Scheidt, *Inorg. Chem., 15* (1976) 3182.
18 W. R. Scheidt, *J. Am. Chem. Soc., 96* (1974) 84.
19 S. E. Eaton and G. R. Eaton, *J. Am. Chem. Soc., 97* (1975) 3660.
20 J. W. Dirks, G. Underwood, J. C. Matheson and D. Gust, *J. Org. Chem., 44* (1979) 2551.